PROBLEMS OF MECHATRONICS
ARMAMENT, AVIATION, SAFETY ENGINEERING

ISSN 2081-5891

5, 1 (15), 2014, 25-40

An Inverse Approach to Estimate Heat Transfer Coefficients of 122 mm Medium-Range Missile During Correction Engine Operation

Janusz ZMYWACZYK*, Piotr KONIORCZYK, Marek PREISKORN, Bogdan MACHOWSKI

Faculty of Mechatronics and Aerospace, Military University of Technology,
2 gen. Sylwestra Kaliskiego St., 00-908 Warsaw, Poland
**corresponding author: e-mail: Janusz.Zmywaczyk@wat.edu.pl*

Manuscript received February 25, 2013. Final manuscript received July 10, 2013

Abstract. This paper presents an inverse approach to estimate the heat transfer coefficients on the inner and the outer sides of a cylindrical shield made of R35 steel containing a gas-dynamic control block of a 122 mm medium-range missile during the combustion of propulsion charge in a correction engine. The specific heat and the thermal diffusivity of R35 steel was experimentally determined using both Netzsch DSC 404F1 Pegasus and LFA 427 measuring devices, respectively. The obtained temperature characteristics of the thermo-physical parameters of cylindrical shield materials were then used to calculate the temperature field concerning the main problem. The inverse problem based on the parameter estimation method using Levenberg–Marquardt optimization procedure was applied to find the unknown heat transfer coefficients. To solve the inverse problem the temperature histories at some locations of the cylindrical shield were known from the experiment.

For this purpose a test measuring stand was built and during the combustion process of the propulsion charge inside the cylindrical shield containing the correction engine the temperature distribution on the outer surface of the cylindrical shield was recorded by means of a high-speed infrared camera (PhantomV210).

A two-dimensional axial-symmetric nonlinear heat conduction model which takes into account the heat loss due to convection and radiation was solved using the Finite Volume Method (FVM). It was found that the assumption of fixed heat transfer coefficients on both sides of the cylindrical shield was sufficient enough to achieve a satisfactory compliance between the measured and the calculated temperature histories at the same location.
Keywords: heat transfer, thermo-physical properties, parameter estimation, R35 steel, heat transfer coefficient

1. INTRODUCTION

Newton's law of cooling describing the quantitatively heat transfer by convection mode in which energy is transferred by diffusion and the bulk motion of fluid is given in Eq. 1

$$\dot{Q} = hA(T_s - T_f) \tag{1}$$

where h[W/m^2/K] is the heat transfer coefficient, A[m^2] is the surface area, T_s, T_f [K, °C] stand for temperatures of the bounded surface and fluid, respectively and $\dot{Q}$ [W] is the convective heat flux.

Despite its simplicity Eq. 1 is very complicated due to the heat transfer coefficients' h dependency on the fluid thermal and mechanical properties within the domain of the boundary layers (hydromechanics and thermal) [1]. The determination of the heat transfer coefficient h is possible for simple problems in an analytical way or by using the correlation formula for the Nusselt number, but for more complex problems more efficient methods are experimental studies of heat and mass transfer problems or the numerical modeling of boundary-value problems. Another approach to determine the heat transfer coefficient may be inverse methods based on the minimization of a mean square functional $S(h)$ involving the measured and the calculated temperatures at the selected locations of the measurement stand. According to Beck [5] coefficient inverse heat conduction problems (CIHCP) can be caused due to the problem of parameter estimation (finding the coefficients of the distribution function in a set of basic functions) or function specification (finding the sought function in a fairly large number of points).

Beck's sequential function specification method with zero-order regularization terms was applied by Buiar and Moura [6] to estimate the convection heat transfer coefficient. Mehta and Jayachandran [7] utilized both the Newton–Raphson method and the sequential future-information method to predict in the wall heat flux, surface temperature, heat transfer coefficient and combustion gas temperature for a typical divergent rocket nozzle in conjunction with the experimentally measured outer surface temperature data during a static test.

The explicit finite difference technique with the nonlinear estimate method and experimentally measured temperature was used by Cheng et al [8] to determine the surface heat transfer coefficient of a steel cylinder with phase transition during gas quenching with high pressure.

The subject of the present study, which refers to [9], is the estimation of the heat transfer coefficients inside a cylindrical shield – h_1 and outside it – h_2, containing the gas-dynamic control block during the combustion of propulsion charge (see Fig. 2). Knowledge of the heat transfer coefficients is essential to calculate the heat fluxes in both radial and axial directions of the analysed component of the missile which are both quite difficult to measure. In addition to this the working temperature of the control unit is limited, hence this work was undertaken to assess the intensity of heat exchange in a specific part of the missile.

2. PROBLEM FORMULATION

2.1. Direct problems

Here is considered that the 2D axial-symmetry transient heat conduction problem in a cylindrical shield of the inner radius r_1, the outer one r_2 and of the height H (see Fig. 3). The thermo-physical properties of the cylindrical shield material are temperature dependent and these are known from the experiment. On both sides of the cylindrical shield heat transfer occurs with constant values of heat transfer coefficients h_1 and h_2, respectively the cylindrical shield is made of R35 steel which is homogenous and isotropic;

- heat transfer is due to the conduction, convection and radiation;
- fluid temperatureT_{f1} inside the cylindrical shield is time dependent and it is equal to the surface temperature of the Gunpowder Pressure Accumulator (GPA) measured at one of these measuring points ($T3$, $T4$, $T5$ – see Fig. 3);
- surfaces of the cylindrical shield and GPA are grey and diffusive and they are considered to be semi-infinite for radiation;
- fluid temperature T_{f2} outside the cylindrical shield is constant and is equal to the ambient temperatureT_0;
- initially at time $t = 0$ there is a homogenous temperature distribution $T_0 = 29.5$°C in the considered domain

The direct heat transfer problem can be written as

$$\rho(T)c_p(T)\frac{\partial T}{\partial t} = \frac{1}{r}\frac{\partial}{\partial r}\left(r\lambda(T)\frac{\partial T}{\partial r}\right) + \frac{\partial}{\partial z}\left(\lambda(T)\frac{\partial T}{\partial z}\right)$$

at $$r_1 < r < r_2,\ 0 < z < H,\ t > 0 \tag{2a}$$

with initial conditions

$$T(r,z;t=0)=T_0 \quad \text{at} \quad r_1 \le r \le r_2,\ 0 \le z \le H \ \text{ and } t=0 \tag{2b}$$

and boundary conditions

$$\lambda(T)\frac{\partial T}{\partial r}=h_1(T-T_{f1})+\varepsilon_1\sigma(T^4-T_{f1}^4) \quad \text{at } r=r_1,\ 0<z<H,\ \ t>0 \tag{2c}$$

$$-\lambda(T)\frac{\partial T}{\partial r}=h_2(T-T_{f2})+\varepsilon_2\sigma(T^4-T_{f2}^4) \quad \text{at } r=r_2,\ 0<z<H,\ \ t>0 \tag{2d}$$

$$\frac{\partial T}{\partial z}=0 \ \text{ at } z=0,\quad r_1<r<r_2,\ \ t>0,\ \ -\lambda(T)\frac{\partial T}{\partial z}=h_1(T-T_{f1}) \ \text{ at } z=H \tag{2e}$$

In order to solve the nonlinear direct problem (Eq. 2) FVM with The Peaceman–Rachford Alternating Direction Implicit (ADI) numerical scheme is used [3]. The right hand side of the boundary conditions (Eqs. 2c, 2d) for a new time step $t_{n+1} = t\,((n+1)\Delta t)$ can be rewritten as

$$h_i(T(t_{n+1})-T_{f,i}(t_{n+1}))+\varepsilon_i\sigma(T^4(t_{n+1})-T_{f,i}^4(t_{n+1}))=(T(t_{n+1})-T_{f,i}(t_{n+1}))\Big/ \left[\frac{1}{h_i+\varepsilon_i\sigma\left(T(t_{n+1})+T_{f,i}(t_{n+1})\right)\left(T^2(t_{n+1})+T_{f,i}^2(t_{n+1})\right)}\right],\ \ i=1,2 \tag{3}$$

Comparing the divider on the right hand side of Eq. 3 with expression 8 on page 255 given during conference proceedings *Thermophysics 2010* [3] one can notice that in this case the heat transfer coefficients (h_e, h_w) of the element conductance K_e and K_w should be replaced by

$$(h_e,h_w)\rightarrow h_i+\varepsilon_i\sigma\left(T(t_{n+1})+T_{f,i}(t_{n+1})\right)\left(T^2(t_{n+1})+T_{f,i}^2(t_{n+1})\right) \tag{4}$$

It is worth mentioning that the solution of the system of algebraic equations resulting from using the Peaceman–Rachford ADI method for each time step t_{n+1} requires iterations due to the non-linearity of the problem. In this case the unknown temperature $T(t_{n+1})$ at iteration ($s = 0$) is replaced by the one from the previous time step t_n, that is

$$T^{(s=0)}(t_{n+1})\leftarrow T(t_n),\ \ T^{(s)}(t_{n+1})\leftarrow T^{(s-1)}(t_{n+1}) \tag{5}$$

The iterative process for the step t_{n+1} is terminated if the following condition is satisfied

$$\left|\frac{T^{(s)}(t_{n+1})-T^{(s-1)}(t_{n+1})}{T^{(s)}(t_{n+1})}\right|\le 0.001,\ \ s=1,2,\ldots,s_{\max} \tag{6}$$

2.2. Inverse problem

The unknown quantities occurring in the direct problem (Eq. 2) are the heat transfer coefficients h_1, h_2. To find them additional information is derived from a real experiment. The inverse problem can be brought up to minimization of the mean square functional S

$$S(h_1, h_2) = J(\mathbf{u}^{\mathrm{T}}) = \sum_{n=1}^{Nt} [T(P, t_n; \mathbf{u}^{\mathrm{T}}) - Y(P, t_n)]^2 \rightarrow \min \tag{7}$$

where

$T(P, t_n; \mathbf{u}^{\mathrm{T}})$ is the model temperature being the solution of the direct problem (Eq. 2) at the same location P and moments t_n as the measured temperatures $Y(P, t_n) = T7(t_n)$ for the currently estimated components of the vector $\mathbf{u}^{\mathrm{T}} = [h_1, h_2]$

Because the gas temperature T_{f1} in the interior of the cylindrical shield was not measured directly it was decided that the temperature T_{f1} was equal to the one of temperatures $T3$, $T4$, $T5$ such that the functional S would reach the smallest value. To solve the inverse problem with respect to the unknown heat transfer coefficients h_1, h_2 the Levenberg–Marquardt optimization method was used and details of the optimization procedure can be found in [3]. However, in this case, to initialize the Levenberg–Marquardt procedure in order to minimize the functional $S(\mathbf{u}^{\mathrm{T}})$ the following starting values were used: $(h_1)^0 = 10$ W/m^2/K, $(h_2)^0 = 5$ W/m^2/K, $\mu_0 = 10^{-3}$, $\delta = 10^{-4}$ (δ – refers to central difference scheme used to calculate sensitivity coefficients).

At each iteration ($iter = 1, 2, \ldots, iter_{\max}$) where $iter_{\max}$ is the final iteration (one must distinguish between the number of iterations for each time step – s from the iteration for the calculation of a new value of the heat transfer coefficients h_i – $iter$), the sensitive coefficients were calculated from the direct problem using a central difference scheme. If the sensitivity coefficients are not correlated to each other then an inverse matrix exists $(\mathrm{X}^{\mathrm{T}}\mathrm{X})^{-1}$ and the unknown parameters can be estimated. The results of the calculation of the reduced sensitivity coefficients ($\beta_{hj} = h_j (\partial T/\partial h_j)$) ($j = 1, 2$) after 6 iterations ($iter = 6$) are depicted in Fig. 1. One can see in Fig. 1b that the reduced sensitivity coefficients β_{hj} reached their extreme values within the measuring time interval $0 \text{ s} < t < 490 \text{ s}$. For the coefficient β_{hj} its maximal value equals 124.4°C at $t = 83$ s and for the coefficient β_{h2} we have (–73.6°C) at $t = 241$ s. Large numerical values of the sensitivity coefficients provide a good numerical conditioning of the inverse problem.

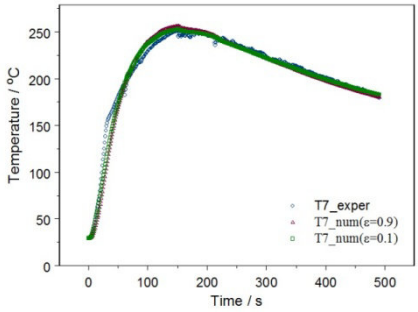

Fig. 1a. Measured and calculated for emissivity $\varepsilon = 0.1$ and $\varepsilon = 0.9$ temperature histories at point $T7$ (see Fig. 3)

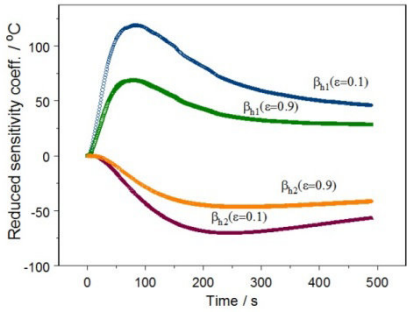

Fig. 1b. Reduced sensitivity coefficients with respect to heat transfer coefficients h_1 and h_2 for emissivity $\varepsilon = 0.1$ and $\varepsilon = 0.9$

3. AN EXPERIMENT AND THERMOPHYSICAL PROPERTIES OF R35 STEEL

3.1. Description of the measuring system for testing the heat exchange

The subject of research is the heat transfer in a central part of a 122 mm medium-range ground to ground missile containing a gas-dynamic control block shown in Fig. 2. This control block enables precise and accurate missile guidance due to control its centre of gravity. The control unit consists of an on-board generator (Gunpowder Pressure Accumulator – GPA) that generates gunpowder gas under appropriate pressure and an actuator equipped with a solenoid valve that separates gases into two nozzles whereby they flow out alternately in radial directions outside the cylindrical shield [4]. The cylindrical shield of a length of H = 360 mm, a diameter of (inner d_1 = 118 mm) and (outer d_2 = 122 mm) is made of R35 steel which is commonly known as AISI 1015 steel. Temperature measurements were made using sheathed K-type thermocouples with an outer diameter of 0.5 mm arranged into seven measurement points as shown in Fig. 3. Temperature histories obtained experimentally are shown in Fig. 4. This figure also show the pressure changes measured in the GPA that occurred within the first 15-17 seconds of the gas generator operation but these results were obtained in a separate experiment. In order to determine the gas velocity in both radial and axial directions the high-speed infrared camera (PhantomV210) capable of recording at 500 Hz full frame rate with a resolution of 800×600 pixels per frame was used. One can notice in Fig. 4 that the temperature of the outer surface of GPA – $T3$ reaches its maximum (about 650°C) at t = 28 s while on the outer surface of the cylindrical shield the temperature $T7$ is equal to 250°C at t = 150 s.

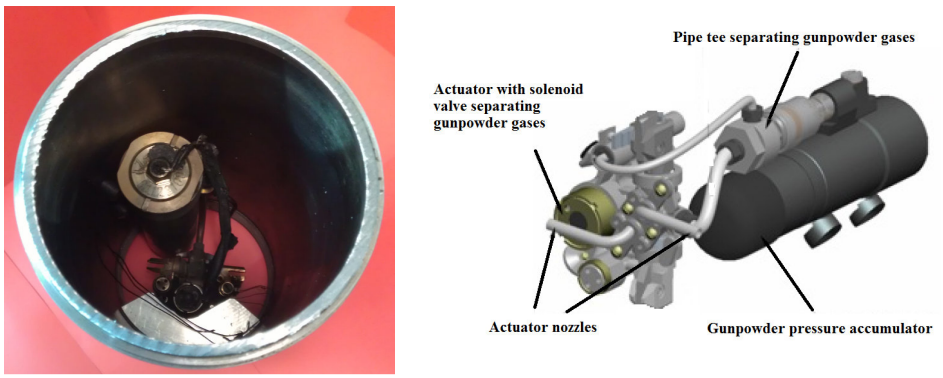

Fig. 2. View of the gas-dynamic control block (left) and its components (right)

The highest temperature $T1$ was recorded close to the nozzle reaching its maximum values twice, namely $T1 = 919°C$ at t = 36 s and $T1 = 982°C$ at $t = 103$ s.

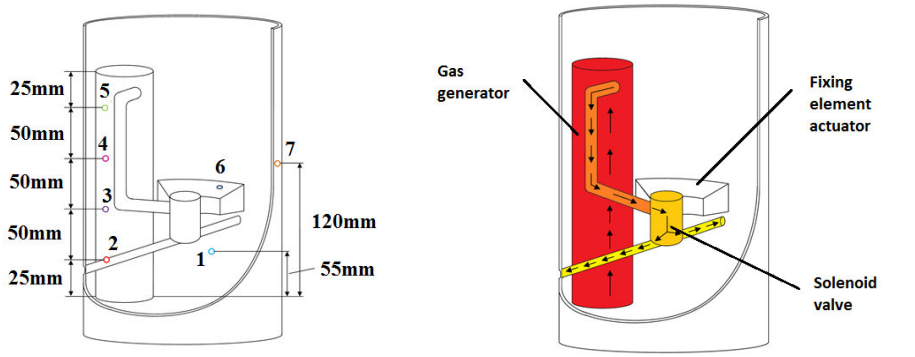

Fig. 3. Arrangement diagram of temperature measurement points (left) and scheme of gas outflow from the correction engine (right) – [10] temperature histories at these points were obtained experimentally (right) – [10]

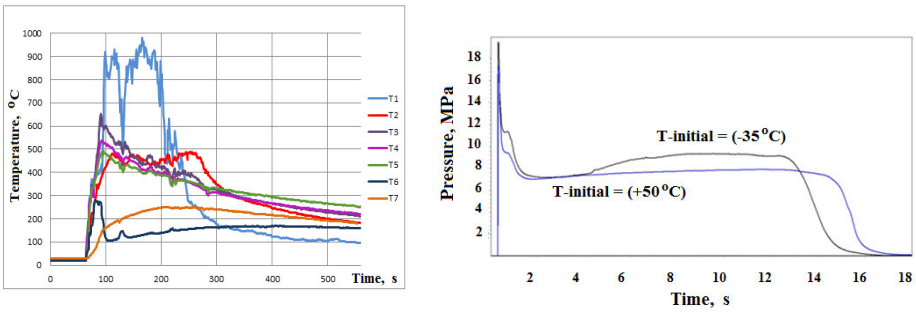

Fig. 4. Temperature at measuring points ($T1$,..,$T7$) (left) and pressure changes in GPA (right) obtained experimentally – [4]

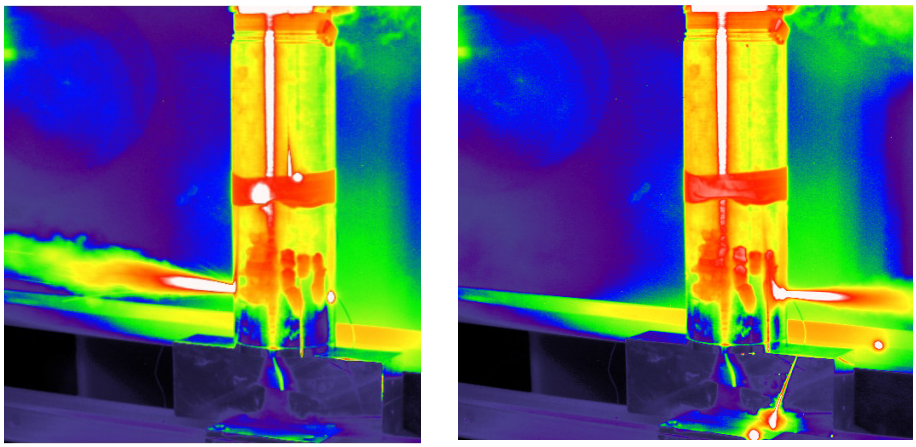

Fig. 5. Thermal image recorded by the infrared camera PhantomV210 during the correction engine operation

The analysis of the thermal image recorded by the infrared camera Phantom V210 (see Fig. 5) allowed the determination of the average gas velocity flowing out from the nozzles and in an axial direction that is equal to 90 m/s and 20 m/s, respectively.

3.2. Measurement of thermo-physical properties of R35 steel

The aim of this study was to determine the differences in temperature characteristics of the specified heat $c_p(T)$ and the thermal diffusivity $a(T)$ between the R35 steel and its literary equivalent AISI 1015 steel. The temperature range of the specific heat investigation was ranged from 320 K up to 1120 K and for the thermal diffusivity from 300 K up to 800 K. Netzsch DSC 404F1 Pegasus and LFA 427 measuring devices were used. The test specimens for measurement of the specific heat and thermal diffusivity were taken from a piece of cylindrical shield just after it cooled down to room temperature, the cylindrical shield was subjected to the correction engine operation shown in Fig. 5.

3.2.1. Thermal diffusivity

The specimen for the thermal diffusivity measurements was made in a form of cylinder with a diameter of d_{dif} = 12.60 mm and a thickness of l = 2.44 mm. To improve laser pulse absorption both faces of the specimen were sprayed with GRAPHIT 33 (~1 μm layer thickness) manufactured by CRC Industries Europe NV.

A typical measurement signal which can be seen on the computer screen corresponding to the sample temperature $T = 69.3°C$ and the laser pulse of a width of 0.6 ms is visible in Fig. 6. To determine the thermal diffusivity of R35 steel at $T = 69.3°C$ which is equal to a = (12.893 ± 0.038) mm^2/s, the Cape–Lehmann with pulse correction theoretical model was chosen giving the best fit among all others available in the LFA 427 software models. The results of the thermal diffusivity investigations of R35 steel are presented in Fig. 7. In addition to this in Fig. 7 the numerical values of thermal diffusivity are shown a (T) of AISI 1015 steel derived from the Temperature Dependent Elastic & Thermal Properties Database MPDB v.7.49.

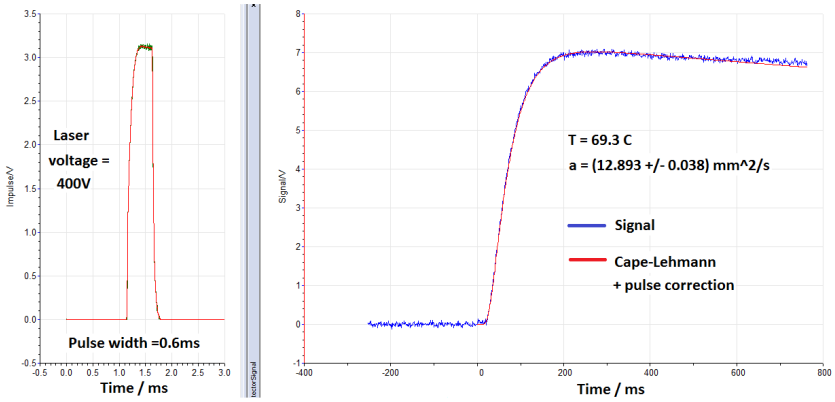

Fig. 6. An example of the measured signals corresponding to thermal diffusivity of R35 steel at T = 69.3°C using Netzsch LFA427 apparatus

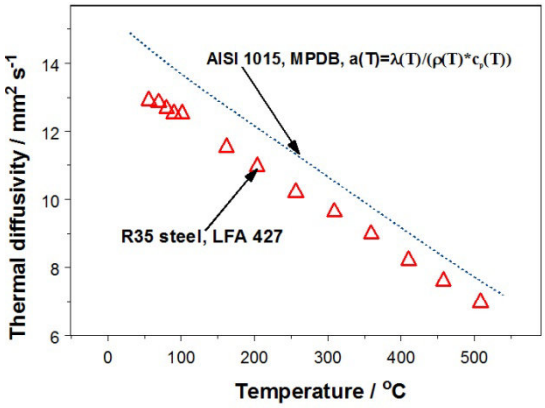

Fig. 7. Thermal diffusivity of R35 steel obtained experimentally using Netzsch LFA 427 apparatus and calculated from MPDB date for AISI 1015 steel

Since the thermal diffusivity of AISI 1015 steel is not available in the MPDB database its numerical values have been calculated using the formula: $a\,(\mathrm{T}) = \lambda\,(\mathrm{T})/[\rho\,(\mathrm{T}) \cdot c_{\mathrm{p}}\,(T)]$ where the temperature characteristics of the thermal conductivity $\lambda\,(\mathrm{T})$, density $\rho\,(\mathrm{T})$ and the specific heat $c_{\mathrm{p}}\,(\mathrm{T})$ have been taken from MPDB.

In Fig. 7 it is easy to notice that the thermal diffusivity temperature characteristics of R35 steel and AISI 1015 steel are almost parallel to each other, the maximum discrepancy of the results amounts to 15%. The numerical values of the thermal diffusivity of R35 steel were obtained experimentally using LFA 427 and were tabulated in [9] and they will not be repeated here.

3.2.2. Specific heat

In the next step, specific heat tests were performed on R35 steel samples. The test specimen with a mass of $m = 167.99$ mg and a density of $\rho = 7.873$ g·cm^{-3} at room temperature ($T = 23$°C) was made in a form of cylinder with a diameter of $d_{\mathrm{Cp}} = 5.0$ mm. The sample was inserted into a platinum-rhodium pan. The values of the specific heat were calculated using the method of 3-curves, i.e. the base line, the reference sapphire and the tested specimen. The heating and the cooling rate were equal to each other and amounted to 10 K/min. Helium was used as an inert gas. The results of the specific heat measurements for R35 steel are shown in [9] but only for the heating period. This time our own calculation procedure for determining the specific heat was used, which takes into a new base signal recording at the end of the measurement. The specific heat $c_{\mathrm{p}}(\mathrm{T})$ is calculated according to the formula given in [11]

$$c_p(T) = \frac{m_{ref}}{m}\frac{\dot{H}(T) - \dot{H}_b(T)}{\dot{H}_{ref}(T) - \dot{H}_b(T)} c_{p,ref}(T) \tag{8}$$

where $\dot{H}_b(T), \dot{H}_{ref}(T), \dot{H}(T)$ stand for the enthalpy fluxes with respect to the base, reference material (sapphire) and the test sample, respectively, m_{ref} and $c_{\mathrm{p,ref}}$ are mass and the specific heat of sapphire, respectively and m is the mass of test specimen. The mass of the reference sapphire was $m_{\mathrm{ref}} = 85.04$ mg. The correlation function of the specific heat for the NBS reference sapphire $c_{\mathrm{p,ref}}(\mathrm{T})$, which values are tabulated by Netzsch within a temperature range from 273.15 K up to 1873.15 K, was chosen in the form

$$\hat{c}_{p,ref}(T[\mathrm{K}]) = a_0 + a_1 T + \frac{a_2}{T^2} + a_3 T^3 + a_4 T^4 + a_5 T^5 + a_6 \ln(T),\ \mathrm{J \cdot g^{-1} K^{-1}} \tag{9}$$

with the coefficients a_i

a_0 = –4.96823635445709
a_1 = –1.82630640547086E-003
a_2 = –1.53532615749585E+003
a_3 = +7.47063054335224E-010
a_4 = –4.28782054156033E-013
a_5 = +7.68617373541201E-017
a_6 = +1.10372836726587

Mean squared error $MSE = \frac{1}{N}\sum_{i=1}^{N}[c_{p,ref}(T_i) - \hat{c}_{p,ref}(T_i)]^2 = 6.8 \cdot 10^{-8}[(\mathrm{J/g/K})^2]$, ($N = 59$) and the maximum discrepancy between the tabulated and approximated values of the specific heat of sapphire using formula (9) is equal to $6.75 \cdot 10^{-4}$ [J/g/K] at $T = 273.15$ K, respectively.

Formula 8 can only be used in such a temperature range where the heating or cooling rate is constant during measurement. Due to the cooling system the maintaining of the assumed cooling rate of 10 K/min was not possible in temperatures ranging from +60°C down to +30°C. In addition to this the results concerning a higher temperature range from 850°C to 900°C were physically unreasonable. For that reason our own results of the specific heat of R35 steel were accepted within temperatures ranging from +60°C up to +850°C both for heating and cooling periods (run 1, 2, 3) of which are shown in Fig. 8.

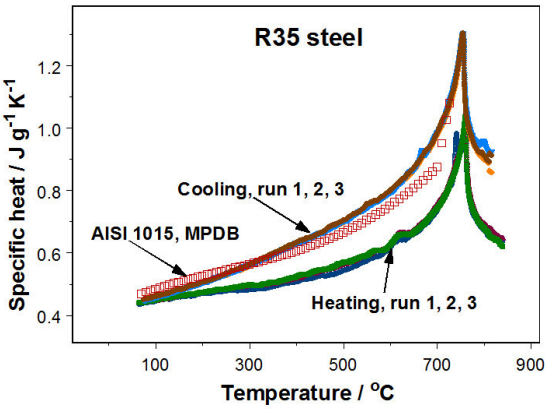

Fig. 8. Comparison of the specific heat of R35 steel own investigations obtained using formula 8 and the one derived from MPDB for AISI 1015 steel

Results of our own specific heat investigations of R35 steel and those corresponding to AISI 1015 steel taken from MPDB v.7.49 which are shown in Fig. 7 indicate the occurrence of the phase transition of the second kind at $T = 754.3$°C, $c_p = 1.302$ $\mathrm{Jg^{-1}K^{-1}}$ for cooling periods and at $T = 759.7$°C, $c_p = 1.046$ $\mathrm{Jg^{-1}K^{-1}}$ for heating periods.

Comparing our results of R35 steel heat investigations with the MPDB values for AISI 1015 steel one can notice in Fig. 8 that the MPDB values are similar to the mean values taken from the heating and cooling runs.

3.2.3. Thermal conductivity

Due to the limitation of only two thermo-physical parameters studies (the specific heat $c_p(T)$ and the thermal diffusivity $a(T)$), the thermal conductivity temperature characteristic $\lambda(T)$ of R35 steel (regarded as an isotropic material) was calculated based on this formula

$$\lambda(T)=\rho(T)c_p(T)a(T)=\frac{\rho(T_0)c_p(T)a_{l_0}(T)}{1+\alpha_V(T)\Delta T}=\frac{\rho(T_0)c_p(T)a_{l_0}(T)}{1+3\alpha_l(T)\Delta T} \tag{10}$$

where $a_{l_0}(T)$ is the thermal diffusivity measured for a sample having a thickness of l_0 at temperature T_0, $\alpha_V(T)$, $\alpha_l(T)$ stands for the thermal expansion and linear thermal expansion coefficients, respectively, $\rho(T_0) = 7873$ kg·m^{-3} is the R35 steel density at a temperature $T_0 = 23$°C, $\Delta T = 1$ K.

Assuming that the linear thermal expansion coefficient $\alpha_l(T)$ of R35 steel is equal to that of $\alpha_l(T)$ of AISI 1015 the temperature characteristic of thermal conductivity was calculated using Eq. 10 and plotted in Fig. 9. During the calculation procedure Eq. 10 mean values (from heating and cooling runs) of the specific heat of R35 steel were accepted.

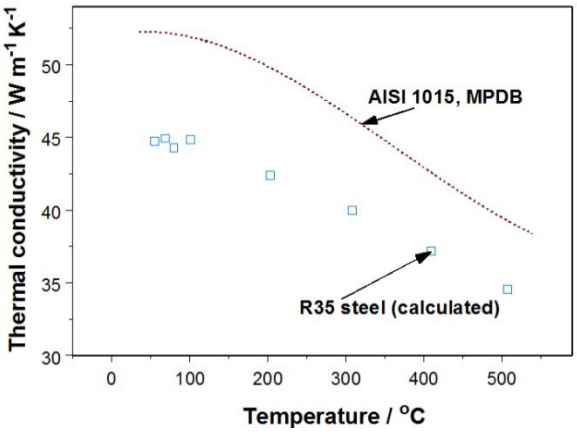

Fig. 9. Thermal conductivity of R35 steel (calculated from Eq. 10) and derived from MPDB for AISI 1015 steel

The results of the thermal conductivity of R35 steel are shown in Fig. 9 and are undervalued by approximately 15% compared to AISI 1015.

4. RESULTS OF HEAT TRANSFER COEFFICIENTS ESTIMATION

The inverse method described in chapter 2 was used to find the unknown convective heat transfer coefficients h_1 and h_2 defined on both sides of the cylindrical shield. It was assumed in this paper that these coefficients would not depend on time. Taking into account radiative boundary conditions (Eqs. 2c, 2d) the total heat transfer coefficient can be treated as the sum of the convective h_i and the radiative $h_{i,r}$ heat transfer coefficients. The results of the parameter estimation of the heat transfer coefficients are shown in Tab.1 for the assumed values of emissivity of cylindrical shield walls $\varepsilon_1 = \varepsilon_2 = \varepsilon$. Analysing the results of the estimation of heat transfer coefficients in Tab. 1 the following conclusions can be drawn:

- the smallest functional value is achieved for $\varepsilon = 0$ ($S = 18331$);
- the higher is value of emissivity the greater is radiative component and the lesser is the convective component of the total heat transfer coefficient;
- the higher the value of emissivity is the lesser the value of the total heat transfer coefficient and the greater is the value of functional S;
- the higher value of emissivity the greater value of the standard deviation $\sigma_{h,i}$ of convective heat transfer coefficients.

Table 1. Heat transfer coefficients estimated values [W/m^2/K]

ε	h_1	$h_{1,r}$	h_1+$h_{1,r}$	σ_{h1}	h_2	$h_{2,r}$	h_2+$h_{2,r}$	σ_{h2}	S
1.0	36.78	27.16	63.94	1.89	25.41	13.01	38.42	1.35	39685
0.9	41.31	24.41	65.72	1.85	27.24	11.69	38.92	1.32	36867
0.5	59.67	13.48	73.15	1.67	34.62	6.43	41.06	1.18	27179
0.3	68.96	8.06	77.02	1.59	38.36	3.84	42.20	1.12	23229
0.1	78.33	2.68	81.01	1.50	42.13	1.27	43.40	1.06	19832
0.0	83.04	0.00	83.04	1.46	44.02	0.00	44.02	1.03	18331

5. DISCUSSION OF THE RESULTS AND CONCLUSIONS

The results of the temperature characteristics of the thermal diffusivity and the specific heat of R35 steel, presented in chapter 3 were compared with AISI 1015 steel derived from MPDB v.7.49.

Based on the obtained data one cannot conclude that R35 differs from AISI 1015 because the chemical composition and the coefficient of linear thermal expansion of the R35 steel had not been investigated. However, the maximum discrepancy in the thermal diffusivity and the specific heat between R35 steel and AISI 1015 was equal to 15%. Having from experiment temperature histories at some locations $T1$,$T7$ it was possible then to solve the inverse problem. The best results in estimating the total heat transfer coefficients using the inverse method were achieved when the radiation was neglected ($\varepsilon = 0$). In this case the estimated values were equal to $h_1 = (83.04 \pm 1.46)$ W/m^2/K and $h_2 = (44.02 \pm 1.03)$ W/m^2/K, respectively.

The results of the inverse solution corresponding to the calculated and measured points at $T7$ temperatures are shown in Fig. 1a. In this figure both the calculated and the measured temperature are consistent to each other and for time greater than 150 s. Before that time there are some differences that are a result from the acceptance of the models fixed values of the total heat transfer coefficients. Such problems will be taken into consideration in the near future by the authors.

ACKNOWLEDGEMENTS

This work was carried out as a part of a development project OR00 0032 08 “122mm precision missile destruction” supported by funds for science in 2009 – 2012. Measurements of thermo-physical properties were performed within the project POIG.02.02.00-14-022/09 “Modernization and construction of new R&D infrastructure of Military University of Technology and Warsaw University of Technology for joint numerical and experimental study of turbine aircraft engines” co-financed by the European Union through the European Regional Development Fund.

REFERENCES

[1] Incropera F.P., Dewitt D.P., Bergman T.L., Lavine A.S., *Fundamentals of Heat and Mass Transfer*, 6-th Ed., John Wiley & Sons, Inc., 2007.

[2] Ozisik M.N., Orlande, H.R.B., *Inverse Heat Transfer, Fundamentals and Applications,* Taylor & Francis, New York, 2000.

[3] Zmywaczyk J., Gapski M., Estimation of thermophysical parameters of stainless steel 1H18N9T by an inverse method, *Proceedings of Thermophysics 2010*, pp. 253-260, Valtice, Czech Republik 2010.

[4] Machowski B. (Ed.), *Final Report of Grant OR00 0032 08, 122 mm Precision-Guided Missile* (in Polish)*,* Warsaw, Poland 2012.

[5] Beck J.V., Blackwell B., Clair S.R.St., *Inverse Heat Conduction*, Ill-Posed Problems, New York, Wiley, 1985.
[6] Buiar C.L., Moura L.M., The sequential method apply to estimate the convection heat transfer coefficient, *Proceedings of Inverse Problems, Design and Optimization Symposium*, Rio de Janeiro, Brazil, 2004.
[7] Mehta R.C., Jayachandran T., Determination of heat transfer coefficient using transient temperature response chart, *Wärme – und Stoffübertragung*, 26, 1-5, 1990.
[8] Cheng H., Xie J., Li J., Determination of surface heat-transfer coefficient of steel cylinder with phase transformation during gas quenching with high pressures, *Computational Materials Science* 29, Issue 4, pp. 453-458, 2004.
[9] Zmywaczyk J., Koniorczyk P., Preiskorn M., Machowski B., Identification of heat transfer coefficient inside a hollow cylinder containing a gas-dynamic control block of medium range ballistic missile, *Proceedings of Thermophysics 2012,* pp. 265-271, Podkylava, Slovak Republic 2012.
[10] Smurawa M., *Analysis of Heat Transfer in a Steel Cylinder Containing the Correction Engine of Combat Missile of Aircraft* (in Polish), M.Sc. Thesis, Military University of Technology, Warsaw, Poland 2012.
[11] Panas A.J., Terpiłowski J., Majewski T., Investigation and complex analysis of 90W-7Ni-3Fe sintered alloy thermophysical properties (in Polish), *Biuletyn WAT*, Vol. LIX, Nr 3, pp. 307-328, 2010.